

Uniaxial pressure dependencies of the phase transitions in GdMnO_3

J. Baier^a, D. Meier^a, K. Berggold^a, J. Hemberger^b, A. Balbashov^c, J.A. Mydosh^a, T. Lorenz^{a,*}

^aII. Physikalisches Institut, Universität zu Köln, Zùlpicher Str. 77, 50937 Köln, Germany

^bExperimentalphysik V, Institut für Physik, University of Augsburg, 86135 Augsburg, Germany

^cMoscow Power Engineering Institute, 105835 Moscow, Russia

Available online 10 November 2006

Abstract

GdMnO_3 shows an incommensurate antiferromagnetic order below $\simeq 42$ K, transforms into a canted A-type antiferromagnet below $\simeq 20$ K, and for finite magnetic fields along the b -axis ferroelectric order occurs below $\simeq 12$ K. From high-resolution thermal expansion measurements along all three principal axes, we determine the uniaxial pressure dependencies of the various transition temperatures and discuss their correlation to changes of the magnetic exchange couplings in RMnO_3 ($R = \text{La}, \dots, \text{Dy}$).

© 2006 Elsevier B.V. All rights reserved.

PACS: 75.47.Lx; 64.70.Rh; 65.40.De; 75.80.+q

Keywords: Multiferroic materials; Magnetoelastic coupling; Rare-earth manganites

GdMnO_3 is one of the multiferroic rare-earth manganites RMnO_3 with $R = \text{Gd}, \text{Tb}$, and Dy where magnetic and ferroelectric order coexist [1]. While for $R = \text{Tb}$ and Dy the multiferroic behavior is already present in zero magnetic field [2], a finite magnetic field along the b axis is necessary to induce multiferroicity in GdMnO_3 . Recently, we have determined the H – T phase diagram for different field orientations by measurements of the uniaxial thermal expansion and magnetostriction along the a , b , and c axis of GdMnO_3 [3]. As shown in Fig. 1, there is a transition from the paramagnetic (PM) to an incommensurate antiferromagnetic phase (ICAFM) around $T_N \simeq 42$ K. For fields above $\simeq 2$ T, the ICAFM transforms into a canted A-type antiferromagnet (cAFM) around $T_c \simeq 20$ K, and a transition to a ferroelectric (FE) phase occurs around $T_{FE} \simeq 12$ K. The notations ‘ICAFM’ and ‘cAFM’ should be treated with some caution, because the magnetic structure of GdMnO_3 has not yet been determined unambiguously.

With increasing field strength, T_N shows a weak, and T_c a moderate, increase while T_{FE} passes through a broad maximum around 7 T. The PM-to-ICAFM transition is of second order, while the other two transitions are of first

order with very strong hysteresis, which is most pronounced in the low-field region [3]. The thermal expansion measurements do not only allow to detect the transition temperatures T_c . Together with specific heat data, it is also possible to determine their dependence on uniaxial pressure p_i via

$$\frac{\partial T_c}{\partial p_i} = V_m \frac{\Delta L_i / L_i}{\Delta S} \quad \text{or} \quad \frac{\partial T_c}{\partial p_i} = V_m T_c \frac{\Delta \alpha_i}{\Delta c}. \quad (1)$$

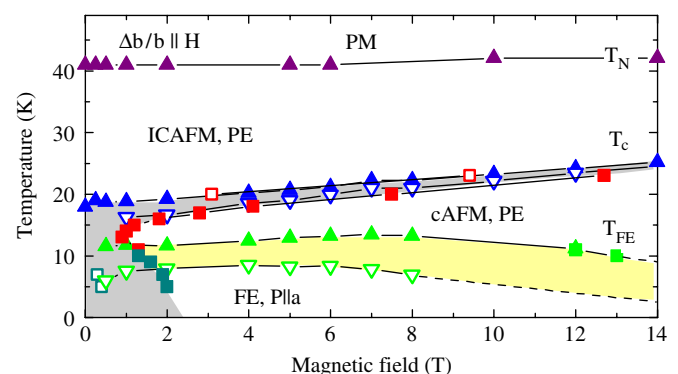


Fig. 1. Phase diagram of GdMnO_3 based on thermal expansion (\blacktriangle, ∇) and magnetostriction measurements (\blacksquare, \square) for magnetic fields applied along the b axis. Filled and open symbols are obtained with increasing and decreasing T or H , respectively. Shaded areas signal regions of strong hysteresis (see also Ref. [3]).

*Corresponding author. Tel.: +49 221 470 3593; fax: +49 221 470 6708.
E-mail address: lorenz@ph2.uni-koeln.de (T. Lorenz).

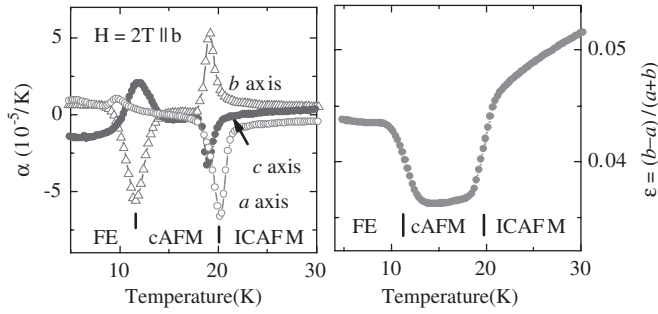


Fig. 2. Left: Thermal expansion of GdMnO₃ along the *a*, *b*, and *c* axes measured in a magnetic field of 2 T parallel to *b*. Right: Orthorhombic distortion calculated via integration of α_a and α_b (see text).

The first expression is the Clausius–Clapeyron and the second one is the Ehrenfest relation, which are valid for first- and second-order phase transitions, respectively. V_m denotes the molar volume, while ΔS and ΔL_i are the respective discontinuous changes of the entropy *S* and the sample length *L_i*. For a second-order transition *S* and *L_i* change continuously, but the specific heat $c = T\partial S/\partial T$ and the thermal expansion coefficients $\alpha_i = 1/L_i \cdot \partial L_i/\partial T$ exhibit jumps at *T_c*.

Fig. 2 displays α_i of the *a*, *b*, and *c* axes. In all three cases a magnetic field of 2 T has been applied along the *b* axis. We have chosen this configuration, because only for fields above $\simeq 2$ T along *b* all three transitions can be observed in GdMnO₃. It would be even better to use a larger field. However, the canted moment of the cAFM phase is parallel to *c*, and the torque $\vec{M} \times \vec{H}$ tends to rotate the sample in fields applied along *b* (or *a*). Along all three axes α_i shows very large anomalies at the ICAFM-to-cAFM and at the cAFM-to-FE transition. The anomalies for the different *i* occur at slightly different temperatures. We suspect that these differences arise from a misorientation of the sample with respect to the field direction. In the transverse configurations, part of the misorientation is due to the above-mentioned torque, since the sample is not completely fixed during the measurement. This problem would hamper a quantitative determination of the pressure dependencies. In the following we will, however, restrict ourselves to a qualitative discussion, since up to now specific-heat data are only available for magnetic fields applied along *c* [4].

Because any ordering decreases *S*, the anomalies ΔS and Δc have positive signs. Thus, the signs of $\partial T_c/\partial p_i$ are determined by the signs of ΔL_i or $\Delta \alpha_i$. A schematic overview of the expected changes of *T_N*, *T_c* and *T_{FE}* under uniaxial pressure along *a*, *b*, and *c* is given in Fig. 3. For *T_N* we used our previous data [3]. The pressure dependencies can be compared to the increasing structural distortion of the GdFeO₃ type as a function of decreasing ionic radius of $R = \text{La}, \dots, \text{Dy}$ in the series RMnO₃ [1,5]. Starting from a cubic perovskite, the GdFeO₃ distortion can be described by a rotation of the MnO₆ octahedra around the *c* axis and a tilt around the *b* axis. As a consequence, the *c* axis continuously decreases and the orthorhombic distortion

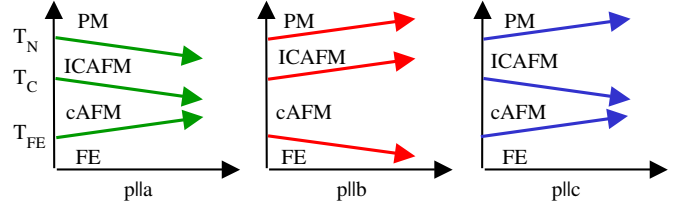


Fig. 3. Dependencies of the transition temperatures of GdMnO₃ on uniaxial pressure along the *a*, *b*, and *c* axis (see text).

$\epsilon = (b-a)/(b+a)$ increases with decreasing radius of *R*. From $R = \text{La}, \dots, \text{Eu}$, *T_N* of the cAFM ordering decreases continuously, while *T_N* of the ICAFM order slightly increases from Gd to Tb and decreases again from Tb to Dy. In a simplified model [5], the decreasing *T_N* until Eu arises from a continuous decrease of the ferromagnetic nearest-neighbor exchange $J_{\text{NN}}^{\text{FM}}$ in the *ab* plane, because of the decreasing Mn–O–Mn bond angle. In addition, the antiferromagnetic next-nearest-neighbor exchange $J_{\text{NNN}}^{\text{AFM}}$ becomes anisotropic. The competition of $J_{\text{NN}}^{\text{FM}}$ and $J_{\text{NNN}}^{\text{AFM}}$ causes the ICAFM order for $R = \text{Gd}, \dots, \text{Dy}$, and certain types of helical magnetic order may induce also a FE ordering [6]. At each transition of GdMnO₃, *p_a* causes the opposite effect as *p_b*. This anti-correlation just reflects the behavior of ϵ . Using the room-temperature lattice constants, we have also calculated $\epsilon(T)$ by integration of α_a and α_b . As shown in Fig. 2, the ICAFM-to-cAFM (cAFM-to-FE) transition causes an abrupt decrease (increase) of ϵ .

Within the above-mentioned model we interpret the uniaxial pressure dependencies as follows: Pressure along *a* increases ϵ and decreases $J_{\text{NN}}^{\text{FM}}$. As a consequence, *T_N* and *T_c* decrease for *p_a*. As discussed already in Ref. [3], the origin of the FE order is not yet clear, but one may speculate that it arises from some kind of helical order, which is induced by a magnetic field along *b*. In this case, it is natural that *T_{FE}* increases for *p_a*, because *p_a* destabilizes the cAFM order and acts in the same direction as the (hypothetical) magnetic-field influence. For pressure along *b*, the same argumentation with inverted signs holds, because ϵ decreases for *p_b*. Since pressure along *c* will mainly shorten the *c* axis, it also acts in the same direction as a decreasing radius of *R*. Therefore, one may expect that *p_c* has a similar influence as *p_a*. In fact, this is the case for the pressure dependencies of *T_c* and *T_{FE}*, but the increase of *T_N* for *p_c* cannot be explained by the above arguments. Up to now we only considered the couplings within the *ab* plane. In order to establish any kind of magnetic ordering from the PM phase, it is, however, necessary to have a finite coupling J_{\perp} along *c*. Thus, we attribute the increase of *T_N* for *p_c* to an increasing J_{\perp} , which overcompensates the influence of the decreasing $J_{\text{NN}}^{\text{FM}}$ due to the increasing distortion.

In summary, we measured the thermal expansion along all three lattice directions of GdMnO₃. From these data we obtained how the transition temperatures of the various phase transitions change under uniaxial pressure, and how

the uniaxial pressure dependencies yield information about the relevant exchange couplings of $RMnO_3$.

This work was supported by the DFG via SFB 608.

References

- [1] T. Goto, et al., Phys. Rev. Lett. 92 (2004) 257201.
- [2] T. Kimura, et al., Phys. Rev. B 71 (2005) 224425.
- [3] J. Baier, et al., Phys. Rev. B 73 (2006) 100402 (R).
- [4] J. Hemberger, et al., Phys. Rev. B 70 (2004) 024414.
- [5] T. Kimura, et al., Phys. Rev. B 68 (2003) 060403 (R).
- [6] M. Mostovoy, Phys. Rev. Lett. 96 (2006) 067601.